

SUPPLEMENTARY MATERIAL

Halaszovich et al.: A human phospholipid phosphatase activated by a transmembrane control module

Supplementary Figure 1. Subcellular localization of other hVSP isoforms

(A) Schematic domain organization of the hVSP1 and hVSP2 splice variants and the hVSP1_{hV2-3N} chimera. hVSP1-3 was previously termed TPIP α (1, 2) or, according to Uniprot (3), TPTE2 isoform 3. Note that this splice variant has a truncated VSD-homologous domain, resulting in only three predicted transmembrane segments, corresponding to S1, S2, and S4 of the full-length variant. hVSP2-3 was previously termed TPTE γ (1) or, according to Uniprot (3), TPTE isoform 3. hVSP1_{hV2-3N} was created by replacing the N-terminus of hVSP1-1 - before the first transmembrane segment - with the corresponding sequence from hVSP2-3 (see *Material and Methods* for details).

(B) Confocal images of CHO or HEK cells co-expressing hVSP variants with the plasma membrane marker Lyn11-GFP. Scale bar, 10 μ m.

hVSP1-3 showed no detectable localization at the plasma membrane (CHO cells). hVSP1-1 was also localized to intracellular compartments in HEK cells, consistent with predominant Golgi localisation as suggested previously for the mouse homolog (4). Replacing the N-terminal mRFP-tag by a C-terminal mRFP did not affect the localization of hVSP1-1 (CHO cells, cf. Fig. 1B). Predominant targeting of hVSP2-3 to the plasma membrane was revealed by strong co-localisation with the plasma membrane marker Lyn11-GFP (CHO cells). Transfer of hVSP2-3's N-terminus to hVSP1-1 does not lead to plasma membrane targeting of the resulting chimeric construct, hVSP1_{hV2-3N} (CHO cells).

(C) Whole-cell voltage-clamp recordings showed absence of sensing currents in cells expressing mRFP-hVSP1-3, consistent with the lack of plasma membrane localization (left panel).

Despite high expression levels (comparable to Ci-VSP, see Fig. 1B) and robust membrane localization, whole-cell voltage-clamp recordings did not reveal any detectable sensing currents in cells expressing mRFP-hVSP2-3 (right panel).

Shown are representative *P*-10 leak-subtracted current traces in response to a voltage step from -100 to +80 mV. Timing of depolarization is indicated in grey.

Supplementary Figure 2. Sensing currents of the hVSP1_{CIV} chimera expressed in *Xenopus* oocytes.

(A) Sensing currents of hVSP1_{CIV} (catalytically inactivated mutant C363S) were measured from *Xenopus* oocytes with the cut-open oocyte method. Traces shown are in response to voltage pulses from -60 to +80 mV in 20 mV increments.

(B) Normalized sensing charge-vs.-voltage (Q-V) curves were derived from the ON sensing currents from experiments as shown in (A). Fits of a two-state Boltzmann distribution to the data (continuous line) yielded potentials at half-maximal charge transfer of 0.0 ± 0.3 mV ($N = 5$) and a sensing charge of $2.16 \pm 0.05 e_0$. Note that activation of the voltage sensor occurs at more negative potentials than in Ci-VSP ($\approx +50$ mV; cf. ref. (5))

For experimental details, see Materials and Methods.

Supplementary Figure 3. hVSP_{CiV}-induced deactivation of KCNQ2/3 currents confirms PI(4,5)P₂ depletion

(A,B) hVSP_{CiV} or its catalytically inactivated mutant C363S were co-expressed with PI(4,5)P₂-sensitive heteromeric KCNQ2/KCNQ3 potassium channels in *Xenopus* oocytes. Traces show representative recordings of KCNQ2/KCNQ3 currents in response to depolarising voltage steps. Holding potential was -90 mV and voltage steps from -80 to +100 mV (20 mV increments) were applied.

Time dependent deactivation of K⁺ currents upon depolarization was only observed in oocytes expressing hVSP_{CiV} (B) but not with the catalytically dead mutant (A), directly demonstrating depletion of PI(4,5)P₂ by hVSP_{CiV}.

(C) Average current amplitudes measured at the end of each voltage step, normalized to current at 0 mV. Data are from 5 oocytes expressing hVSP_{CiV} or hVSP_{CiV}(C363S), each.

Supplementary Figure 4. PI(3,4,5)P₃ is a substrate for the 5-phosphatase hVSP1_{CiV}.

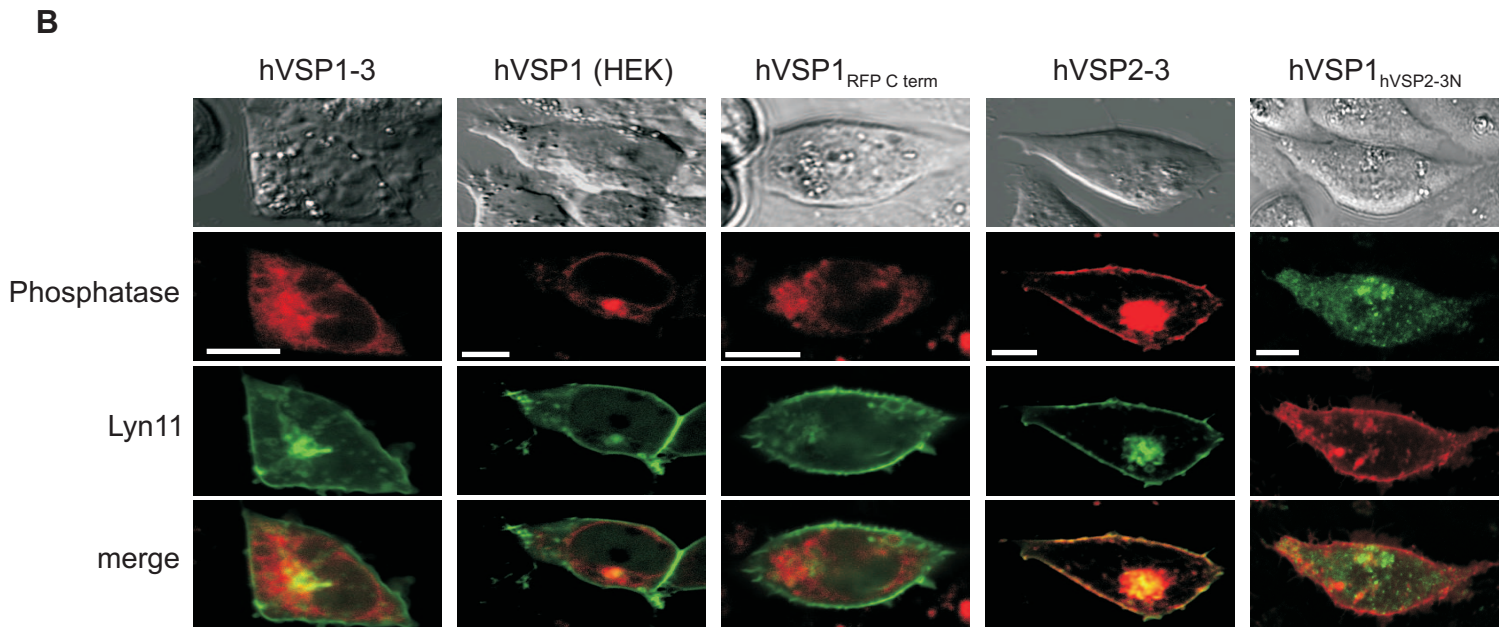
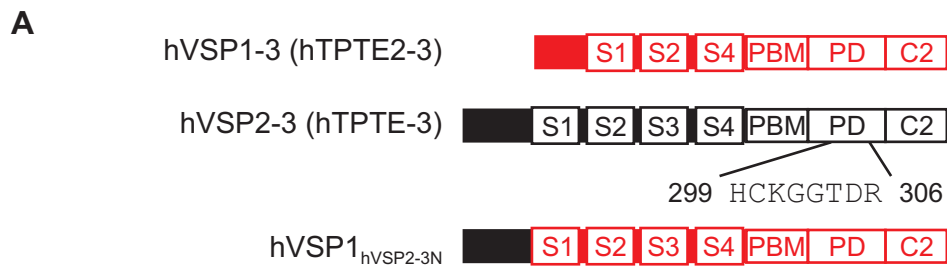
(A) Averaged TIRF fluorescence signals from single CHO cells co-expressing mRFP-hVSP1_{CiV} with the PI(3,4,5)P₃ sensor PH_{Btk}-GFP and the constitutively active PI3-kinase p110 α (K227E) (6). Cells were whole-cell voltage-clamped at -100 mV for at least 3 min and then subjected to a step depolarization to +80 mV (timing indicated by grey region). Note that depolarization-induced decrease of fluorescence indicates dissociation of the sensor domain from the membrane, and thus depletion of PI(3,4,5)P₃.

(B) Same experiment as in (A) but with the PI(3,4)P₂ sensor PH_{TAPP1}-YFP. Note that increase of fluorescence indicates production of PI(3,4)P₂, consistent with dephosphorylation of PI(3,4,5)P₃ at the 5 position by hVSP1_{CiV}.

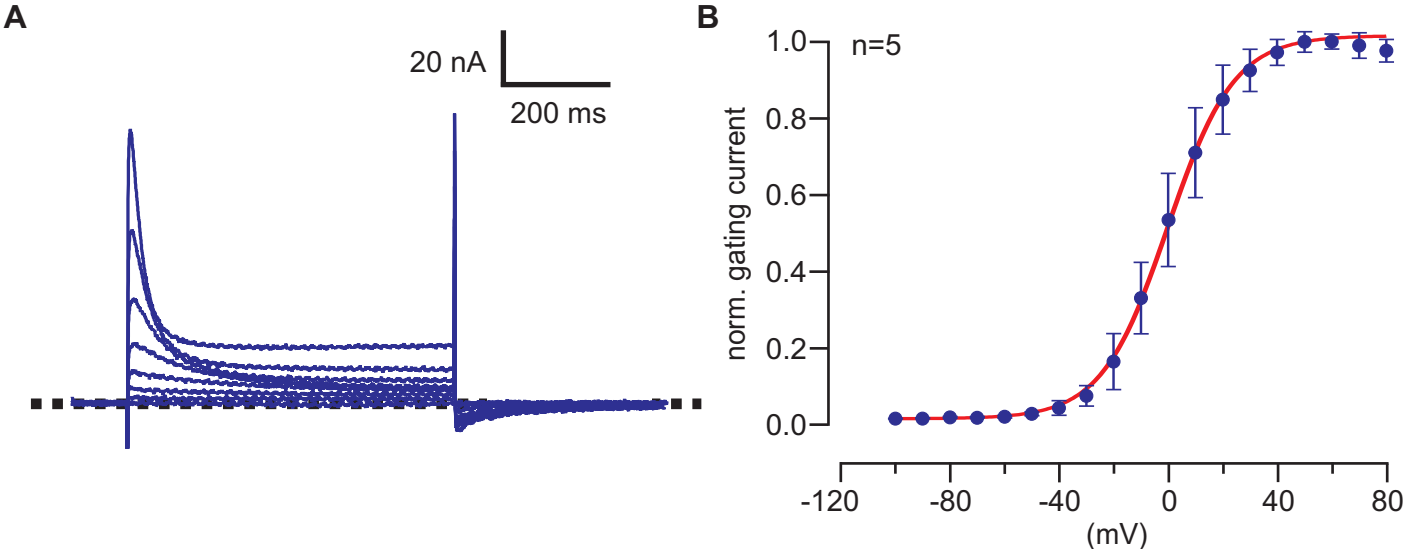
References

1. Tapparel, C., A. Reymond, C. Girardet, L. Guillou, R. Lyle, C. Lamon, P. Hutter, and S. E. Antonarakis. 2003. The TPTE gene family: cellular expression, subcellular localization and alternative splicing. *Gene* **323**: 189-199.
2. Walker, S. M., C. P. Downes, and N. R. Leslie. 2001. TPIP: a novel phosphoinositide 3-phosphatase. *Biochem J* **360**: 277-283.
3. Jain, E., A. Bairoch, S. Duvaud, I. Phan, N. Redaschi, B. E. Suzek, M. J. Martin, P. McGarvey, and E. Gasteiger. 2009. Infrastructure for the life sciences: design and implementation of the UniProt website. *BMC Bioinformatics* **10**: 136.
4. Wu, Y., D. Dowbenko, M. T. Pisabarro, L. Dillard-Telm, H. Koeppen, and L. A. Lasky. 2001. PTEN 2, a Golgi-associated testis-specific homologue of the PTEN tumor suppressor lipid phosphatase. *J Biol Chem* **276**: 21745-21753.
5. Villalba-Galea, C. A., W. Sandtner, D. M. Starace, and F. Bezanilla. 2008. S4-based voltage sensors have three major conformations. *Proc Natl Acad Sci U S A* **105**: 17600-17607.
6. Halaszovich, C. R., D. N. Schreiber, and D. Oliver. 2009. Ci-VSP is a depolarization-activated phosphatidylinositol-4,5-bisphosphate and phosphatidylinositol-3,4,5-trisphosphate 5'-phosphatase. *J Biol Chem* **284**: 2106-2113.

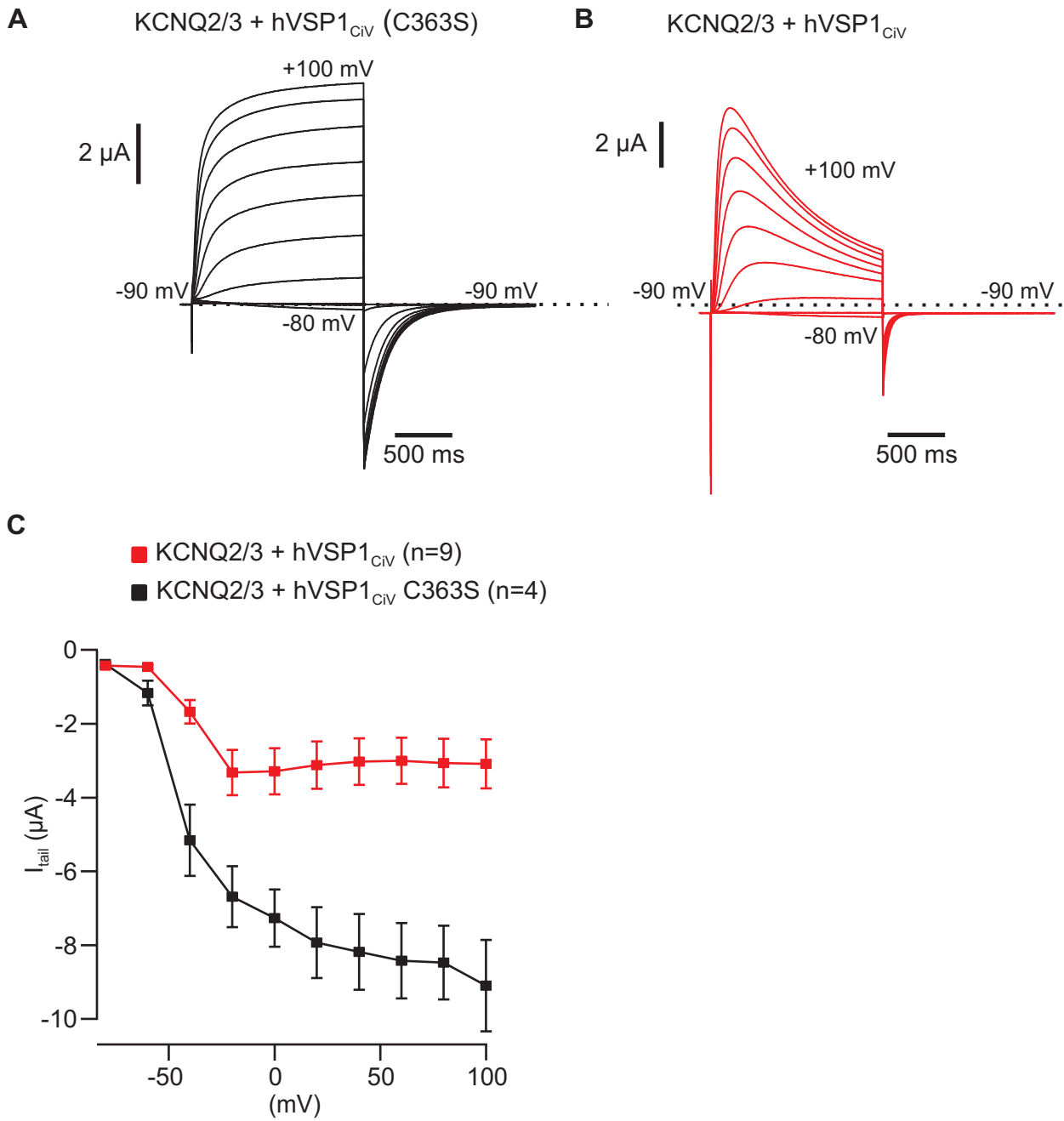
Supplementary Figure 1



Supplementary Figure 2



Supplementary Figure 3



Supplementary Figure 4

